International Journal of Research and Review
www.ijrrjournal.com E-ISSN: 2349-9788; P-ISSN: 2454-2237

Original Research Article

Spin Polarization of fcc Ni_n (100) and (111) Surfaces with GGA and GGA+U

Yousif Shoaib Mohammed[1,2,3]

[1]Department of Physics, College of Science & Art, Qassim University, Oklat Al- Skoor, P.O.Box: 111, Saudi Arabia.
[2]Department of Physics, College of Education, Dalanj University, Dalanj, Sudan
[3]Physics Department, Africa City for Technology, Khartoum, Sudan

Received: 13/03/2015 *Revised: 16/04/2015* *Accepted: 17/04/2015*

ABSTRACT

Results are presented of a first-principle calculation of the Density Functional Theory (DFT) ferromagnetic (FM) face-centered cubic (fcc) of Nickel Ni_n (100) and (111) surfaces for n = 3, 5 and 7 layers. The relaxed and non-relaxed electronic structures of both surfaces are determined with generalized gradient approximation (GGA) and generalized gradient approximation + Hubbard (GGA+U). The observed trends can be explained as in earlier studies in terms of the hybridization between d states of Ni substrate, also some interesting specific behavior of the magnetization in the fcc Ni (100) and (111) surfaces with different layers has been observed.

Keywords: Surface; magnetic moments; relaxation; DOS; Ni

INTRODUCTION

Feed In this research, the results of the systematic theoretical study of the magnetic properties of fcc (100) and (111) surfaces of ferromagnetic metal Ni_n are presented for n = 3, 5, and 7 layers. We have calculated the magnetic moment through the interface region including that of the topmost Ni layer. In our calculations the size of the magnetic moment and total energies for several layers of fcc (100) and (111) Ni surfaces have been considered.

For instance, the results of Pt clusters on Pt (001) using the embedded atom model (EAM) method, [1] agreed with the results of field-ion microscopy (FIM) in predicting that clusters oscillate between chain and island-type configurations as the number of adatoms increases from three to six; [2] and the predictions for the most stable structures of small Pt clusters on Pt (111) using the VC EAM agrees with few exceptions. [3] While the geometries observed in FIM studies of Ir clusters on Ir (111). [4]

We know that the ferromagnetic properties of transition metals based on an imbalance between the number of spin-up and spin-down electrons. This is reflected in the electronic structure by splitting of their energy bands, which results in more spin-up (majority) and spin-down (minority) occupied states. In Ni, for example, this

gives rise to a net magnetic moment per atom of 0.591 μB [5] and of 0.61 μB [6] consequently, the partly occupied, hence truly magnetic.

Ordinary photoemission experiments have detected surface state just below the Fermi energy E_F on Ni (111) [7] and Ni (001), [8] leaving the spin character undetermined. An occupied surface state on Ni (110) was observed as a double peak structure and interpreted as spin-split majority and minority spin states. [9]

Surface magnetism can be very different from the one in the bulk, [10] because the electronic structure of the surface is often very different. By studying surface magnetism one can gain insight into certain aspects of the surface electronic structure, especially spin polarization, which is linked to the density of states (DOS) of majority and minority electrons. Ion beams at keV energies and grazing incidence have an extreme sensitivity to the surface region. [11] The electron capture spectroscopy (ECS) used for studying surface magnetism of Fe (110) and Ni (110), where it was shown that the surface spin polarization is due to a higher density of states for the majority electrons at the Fermi energy. [12] In which they found that Ni (110) have a much higher density of states for minority than for majority electrons at the Fermi energy as calculations [13-15] predict, which is supported by early studies using capture of electrons into the ground state of deuterium atoms and subsequent analysis of the polarization via a nuclear scattering reaction. [16]

The enhancement of magnetic moment at the surfaces of transition metals is a well established fact. [14,17] Development in experimental techniques along with extremely accurate first-principles, self-consistent local spin-density (LSDA) based calculations have only strengthened this belief. This enhancement is attributed to the reduced symmetry and coordination number at surfaces. This in turn results in band narrowing and hence enhancement of the paramagnetic density of state at EF. [18] Stoner-like arguments then lead to an enhancement of the local magnetic moment. Thought in general it is true that band narrowing leads to enhancement of the surface magnetization.

In discussing surface enhancement the role of d-band is often emphasized. The s and p bands play a significant role, especially in Ni (100) and hexagonal closed packed (hcp) Co (100) surfaces, where the enhancement is feeble. [19] Also they found that the moment enhancement is largest in Fe bcc (100), where the majority band (in bulk) is not saturated and less in Ni and Co where the majority band is almost saturated. In addition to that, the less saturated majority band in bulk leads to the more possibility of enhancement at the surface. [20] For Ni thin films, almost the whole of the enhancement at the surface was due to the dx^2-y^2 orbital, but for this state the majority band was more saturated than the three t_{2g} states in the bulk.

From a theoretical point of view, there have been numerous studies of thin films and surfaces, both for free standing thin films, as well as for those on substrates, using different methods, i.e. (i) Single slab geometry with boundary matching Green functions. [21,22] (ii) Slabs in a three-dimensional super cell, well separated by empty space with charge but no atoms. [23] The assumption is that the slabs separated by sufficiently wide empty spaces do not interact with one another. (iii) A green function technique making use of the two-dimensional periodicity on flat surfaces and treating the direction perpendicular to the surface by a real-space method. [24]

The purpose of this paper is to carry out a detailed orbital resolved study of magnetic moments and DOS on both Ni

(100) and (111) surfaces with GGA and GGA+U.

COMPUTATIONAL METHODS

All calculations have been performed with VASP (Vienna ab initio Simulation Package), [25-29] a first principles plane-wave code based on spin-polarized density functional theory. The interaction between ions and valence electrons was described by the projector augmented-wave (PAW) method. [30] The Kohn-Sham equations were solved via iterative matrix diagonalization based on the minimization of the norm of the residual vector to each eigenstate and optimized charge- and spin-mixing routines. [31-33]

The generalized gradient corrections added in form of Perdew-Wang functional PW91 [34] were chosen for the exchange correlation function for the GGA. The spin interpolation of Vosko et a1 was also used. [35] To correct the strong electronic correlation, a simple rotationally invariant DFT+U version proposed by Dudarev et a1 [36] and implemented in VASP [37] was used as GGA+U. In this method, the parameters U and J did not enter separately, only the difference U-J was meaningful. Parameters U and J represented on-site Coulomb interaction energy and exchange energy respectively. J was kept to 1 eV, and a value of U-J=2.4 eV [5,38] was used in our calculations. A detailed description of the DFT+U method can be found in Ref. [39]

All results reported in this research were carried out on a surfaces face-central-cubic ferromagnetic supercell including Ni_n (100) and (111) orientations for n = 3, 5, and 7 layers. Convergence tests have been checked carefully both for plane wave cutoff energy and k points sample, a plane-wave set expanded in energy cutoff 270 eV and k-points sample with a mesh of points 9x9x1 generated by the scheme of Monkhorst and Pack [40] can ensure the total energies difference is less than 3 meV/atom. For total energy and DOS calculation, the integration over the Brillouin zone was performed using the linear tetrahedron method with blochl corrections. [41-43]

RESULTS AND DISCUSSION

A number of first-principles calculations based on slab models were reported on the electronic and magnetic properties of Ni surfaces. [44,45,14] The change in the first interlayer spacing Δ_{12}, was also investigated both experimentally [46] and computationally [15] and was found to be a few percent. In our calculations, the surface relaxations change magnetic moments only of the order of 0.1%. Hence we will show hereafter calculated results for relaxed and non-relaxed Ni_n (100) and (111) surfaces for n = 3, 5 and 7 layers.

In this study we used the lattice constants of our previous DFT bulk Ni calculations, [5] which produce a ferromagnetic solution with lattice constant, magnetic moment, and bulk modulus of 3.53 Å, 0.591 μB and 188.6 GPa for GGA, while for GGA+U (U-J = 2.4 eV) the obtained values are 3.51 Å, 0.659 μB, and 178.3 GPa respectively. Tables 1, show us the charge profile of the relaxed and non-relaxed orbital in various layers for a seven-layer slab Ni (100) with GGA and GGA+U respectively. It shows that the charge-density oscillates with layers. The GGA+U calculations show the enhancement of the charge due the strong correlations. Other crystallographic orientation is also considered. The charge profile of the relaxed and non-relaxed orbital for seven-layer slab Ni (111) with GGA and GGA+U are given in Tables 2 respectively. Similar behaviors of slab Ni (100) are obtained. The magnetic moments of seven-layers of Ni (100) and (111) slabs are reflected in Fig. 1, which shows that the magnetic moments oscillatory decreases from the surface layer (S) to the central layer (C) toward the bulk value.

Table 1: The GGA and GGA+*U* (*U-J* = 2.4 eV) atomic sphere charge of seven-layer slab Ni (100) with and without relaxation. Surface (S) atoms. S-1 and S-2 denote the first and second atomic layers below the surface atoms, and C labels to the atom in the Center of the film.

Layer			s	p	d	Total
GGA	Non-relaxed	S	0.527	0.403	8.443	9.374
		S-1	0.559	0.596	8.472	9.627
		S-2	0.563	0.600	8.480	9.643
		C	0.563	0.598	8.473	9.633
	Relaxed	S	0.539	0.424	8.465	9.428
		S-1	0.566	0.610	8.473	9.650
		S-2	0.560	0.591	8.465	9.616
		C	0.562	0.596	8.475	9.633
GGA+*U* (*U-J* = 2.4 eV)	Non-relaxed	S	9.428	0.382	8.530	9.430
		S-1	9.650	0.575	8.546	9.674
		S-2	9.616	0.578	8.540	9.676
		C	9.633	0.577	8.542	9.678
	Relaxed	S	0.529	0.403	8.541	9.473
		S-1	0.559	0.590	8.550	9.699
		S-2	0.554	0.569	8.539	9.663
		C	0.558	0.577	8.543	9.678

Table 2: The GGA and GGA+*U* atomic sphere of seven-layer slab Ni (111) with and without relaxation.

Layer			s	p	d	Total
GGA	Non-relaxed	S	0.553	0.456	8.448	9.457
		S-1	0.557	0.596	8.471	9.624
		S-2	0.565	0.600	8.466	9.630
		C	0.563	0.600	8.466	9.629
	Relaxed	S	0.556	0.463	8.447	9.466
		S-1	0.560	0.602	8.463	9.634
		S-2	0.564	0.597	8.466	9.626
		C	0.561	0.597	8.478	9.637
GGA+*U* (*U-J* = 2.4 eV)	Non-relaxed	S	0.546	0.439	8.504	9.490
		S-1	0.556	0.584	8.524	9.654
		S-2	0.561	0.583	8.550	9.694
		C	0.560	0.585	8.547	9.692
	Relaxed	S	0.550	0.446	8.520	9.516
		S-1	0.559	0.592	8.519	9.671
		S-2	0.560	0.580	8.547	9.687
		C	0.558	0.582	8.528	9.668

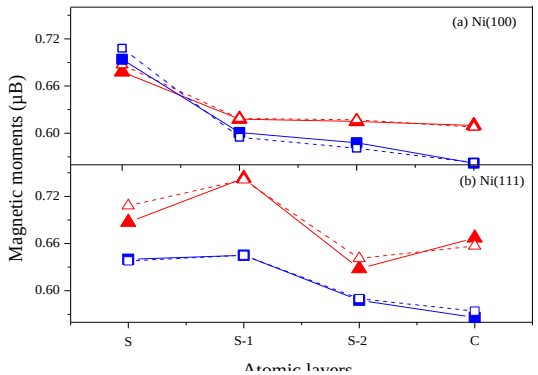

Fig. 1: Oscillatory magnetic moments of seven-layers for (a) Ni (100) (b) Ni (111) slabs. Solid symbols straight lines for relaxed and open symbols dashed lines for non-relaxed. Square for GGA and triangle for GGA+*U* respectively.

Tables 3 and 4, shows us the magnetic moments for different numbers of relaxed and non-relaxed layers of Ni (100) and (111) with GGA and GGA+U respectively. From these tables we see that the surface magnetic moment of layer oscillatory increases with increasing the number of layers. While the magnetic moments of the atoms in the center of the films oscillatory decreases with increasing the number of layers towards the bulk value. However, it is the manner in which the charge redistribution takes place among the five d orbital, which makes surface magnetization different from bulk. Our estimate of the enhancement of the surface magnetic moment agrees closely with the result of Alden. [18] Fig. 2 reflected the calculation of the total energies for different

number of layers for Ni (100) and (111) slabs. The figure shows that the GGA results are more stable than the GGA+U for relaxed and non-relaxed cases.

Table 3: The GGA and GGA+*U* Magnetic moments of fcc Ni_n (100) for n = 3, 5, and 7 layers with and without relaxation.

	n	non-relaxed				relaxed			
		C	S	S-1	S-2	C	S	S-1	S-2
GGA	3	0.594	0.694			0.559	0.673		
	5	0.594	0.697	0.582		0.584	0.691	0.595	
	7	0.563	0.708	0.595	0.581	0.562	0.694	0.601	0.588
GGA+*U*	3	0.660	0.732			0.616	0.702		
	5	0.665	0.748	0.629		0.657	0.729	0.674	
	7	0.608	0.687	0.619	0.617	0.610	0.678	0.618	0.615

Table 4: The GGA and GGA+*U* Magnetic moments of fcc Ni_n (111) for n = 3, 5, and 7 layers with and without relaxation.

	n	non-relaxed				relaxed			
		C	S	S-1	S-2	C	S	S-1	S-2
GGA	3	0.687	0.651			0.695	0.640		
	5	0.573	0.609	0.614		0.574	0.608	0.615	
	7	0.574	0.638	0.645	0.590	0.566	0.640	0.645	0.588
GGA+*U*	3	0.763	0.651			0.785	0.684		
	5	0.615	0.609	0.721		0.605	0.667	0.732	
	7	0.657	0.638	0741	0.641	0.667	0.687	0.743	0.628

Fig. 3 shows the layer projected local density of states (LDOS) for a seven-layer slab Ni (100) for non-relaxed GGA and GGA+U respectively. The surface layer shows the characteristic narrowing, while the central layer resembles that of the bulk. [5]

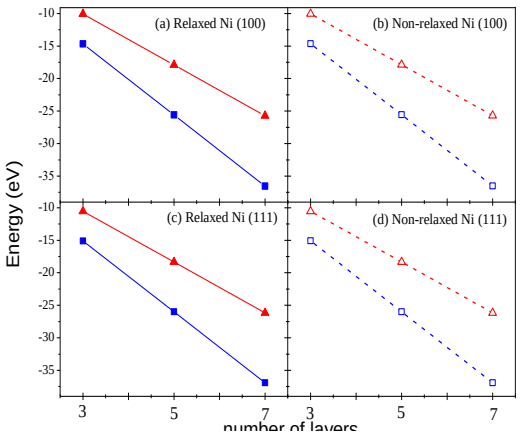

Fig. 2: Calculated total energy for different layers of Ni (100) and (111) slabs. Square for GGA and triangle for GGA+*U* respectively. Solid and dashed lines for relaxed and non-relaxed respectively. Bulk value from ref. [5]

The values of LDOS are (states/atom.eV). Other crystallographic layer projected LDOS are also considered for slab Ni (111) with relaxed GGA and GGA+U, the result is reflected in Fig. 4. Similar behaviors of slab Ni (100) are obtained. Our measurements of the LDOS show that in slab Ni (100) and (111) the minority electrons have a higher density of states at the Fermi energy than majority electrons for all cases studied (see Figs. 3 and 4) in a good agreement with Ni (110) surface works [12,13] predicted. An interesting facet of this study is the steep suppression of the magnetic moment for the atoms below the surface layer (see Fig. 2) Similar behavior was found and reported in. [19,22]

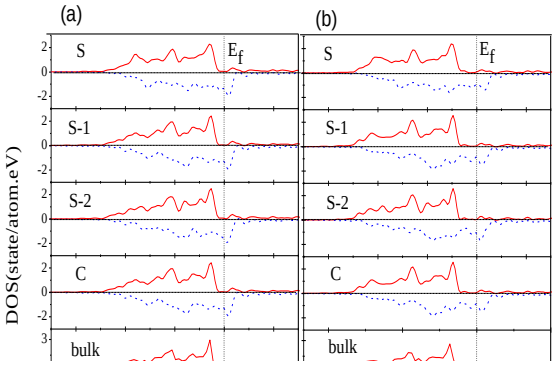

Fig. 3: Non-relaxed LDOS of seven-layer Ni (100) for (a) GGA and (b) GGA+U. (E_f) is Fermi energy. Red solid and blue dotted lines for spin-up and spin-down respectively.

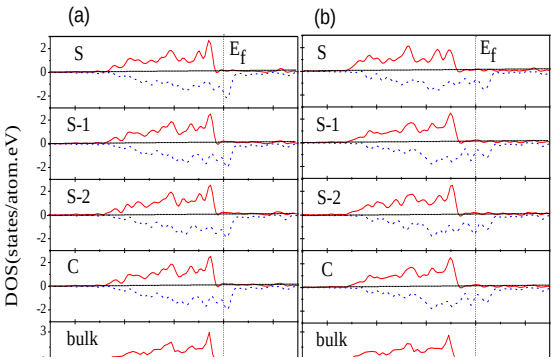

Fig. 4: Relaxed LDOS of seven-layer Ni (111). (a) GGA and (b) GGA+U. (E_f) is Fermi energy. Bulk value from ref. [5]

CONCLUSION

The main points of our study can be summarized as following:

1- Oscillatory magnetic moments and charges in all cases studied were observed.

2- Ni (100) and (111) surfaces magnetic moments enhancement attributed to the reduced symmetry and coordination number at surfaces.

3- The relaxed and non-relaxed surface local magnetic moments of Ni (100) and (111) oscillatory increase with increasing the number of layers, and the local magnetic moments of the atom in the center of the films oscillates decrease towards the bulk value.

4- When strong correlation is included, the magnetic moments of Ni (100) and (111) surfaces increased.

5- Ni (100) and (111) surfaces have a much higher density of states for minority than for majority electrons at the Fermi energy, agrees with Ni (110) surface works [12,13] predicted.

ACKNOWLEDGEMENTS

I would like to thanks African City for Technology, Khartoum – Sudan so much.

REFERENCES

1. Schwoebel P R, Foiles S M, Bisson C L, and Kellogg G L, Structure of platinum adatom clusters on Pt(100): Experimental observations and embedded-atom-method calculations, Phys Rev B 1989; 40: 10 639.
2. Foiles S M, Baskes M I, and Daw M S, Embedded-atom-method functions for the fcc metals Cu, Ag, Au, Ni, Pd, Pt, and their alloys, Phys Rev B, 1986; 33: 7983.
3. Fallis M C, Daw M S and Fong C Y, Energetics of small Pt clusters on Pt(111): Embedded-atom-method calculations and phenomenology, Phys. Rec. B, 1995; 51: 7817.
4. Wang S C and Ehrlich G, Structure stability and surface diffusion of clusters: Irx on Ir(111), Surf. Sci., 1990; 239: 301.
5. Yousif Shoaib Mohammed, Yu Yan, Hong xia Wang, Kai Li, Xiao bo Du, Stability of Ferromagnetism in Fe, Co, and Ni Metals under High Pressure with GGA and GGA+U, Journal of Magnetism and Magnetic Materials, 2010; 322: 653.
6. Moroni E G, Kresse G and Hafner J, Ultrasoft pseudopotentials applied to magnetic Fe, Co, and Ni: From atoms to solids, Phys. Rev. B, 1997; 56: 15629. Dennilson B, Eric l P and Stanleg M, Polymorphism of Iron at High Pressure, J. Appl. Phys., 1956; 27: 291.
7. Himpsel F J and Eastman D E, Observation of a L_1-Symmetry Surface State on Ni(111), Phys. Rev. Lett., 1978; 41: 507.
8. Pummer E W and Eberhardt W, A temperature-dependent study of the magnetic surface states on Ni(100) near the Fermi level, Phys. Rev. B, 1979; 20: 1444, and Erskine J L, Surface States and the Photoelectron Spin Polarization of Ni(100), Phys. Rev. Lett., 1980; 45: 1446.

9. Eberhardt W, Plummer E W, Horn K and Erskine J L, Magnetic Exchange Splitting of Electronic Surface States on Ni(110), Phys. Rev. Lett., 1980; 45: 273.
10. Freeman A J and Wu R Q, Electronic Structure Theory of Surface, Interface and Thin Film Magnetism, J. Magn. Magn. Mater., 1991; 100: 497.
11. Winter H, Collisions of atoms and ions with surfaces under grazing incidence, Phys. Rep., 2002; 367: 387 and Niehus H, Heiland W and Taglauer E, Low-Energy Ion Scattering at Surfaces. Surf. Sci. Rep., 1993; 17: 213-218.
12. Unipan M, Winters D F A, Robin A, Morgenstern R, Hoekstra R, Surface spin polarization in Fe(1 1 0) and Ni(1 1 0), NIM B, 2005; 230: 356.
13. Moruzzi V L, Janak J F, Williams A R, in: Calculated Electronic Properties of Metals, Pergamon Press, New York, 1978; 168 and 180.
14. Wimmer E, Freeman A J, Krakauer H, Magnetism at the Ni(001) surface: A high-precision, all-electron local-spin-density-functional study, Phys. Rev. B, 1984; 30: 3113.
15. Mittendorfer F, Eichler A and Hafner J, Structural electronic and magnetic properties of nickel surfaces, Surf. Sci., 1999; 423: 1.
16. Rau C, J. Magn. Magn. Mater., Electron spin polarization esp at surfaces of ferromagnetic metals, 1982; 30: 141.
17. Wang C S, Freeman J A, Surface states, surface magnetization, and electron spin polarization: Fe(001), Phys. Rev. B, 1981; 24: 4364.
18. Aldén M, Mirbt S, Skriver H L, Rosengaard N M and Johansson B, Surface magnetism in iron, cobalt, and nickel. Phys. Rev. B, 1992; 46: 6303-6312.
19. Chakraborty M, Mookerjeea A and Bhattacharya A K, Magnetism in surfaces: an orbital-resolved study, Journal of Magnetism and Magnetic Materials, 2005; 285: 210-223.
20. Olle Eriksson, Fernando G W, Albers R C, Boring A M, Enhanced orbital contribution to surface magnetism in Fe, Co, and Ni, Solid State Commun., 1991; 78: 801.
21. Wang C S, Freeman A J, Surface states, surface magnetization, and electron-spin polarization: Ni(001), Phys. Rev. B, 1980; 21: 4585.
22. Jepsen O, Madsen J, Andersen O K, Spin-polarized electronic structure of the Ni(001) surface and thin films, Phys. Rev. B, 1982; 26: 2790.
23. Alldredge G P and Kleinman L, New Method of Calculating Bulk and Surface States in Thin Films, Phys. Rev. Lett., 1972; 28: 1264.
24. Skriver H L and Rosengaard M N, Self-consistent Green's-function technique for surfaces and interfaces, Phys. Rev. B, 1991; 43: 9538.
25. Kresse G and Hafner J, Ab initio molecular dynamics for liquid metals, Phys Rev B, 1993; 47: 558.
26. Kresse G and Hafner J, Ab initio molecular-dynamics simulation of the liquid-metal-amorphous-semiconductor transition in germanium, Phys Rev B, 1994; 49: 14251.
27. Kresse G and Furthmüller J, Efficient iterative schemes for ab initio total-energy calculations using a plane-wave basis set, Phys Rev B, 1996; 54: 11169.
28. Kresse G and Furthmüller J, Efficiency of ab-initio total energy calculations for metals and semiconductors using a plane-wave basis set, Comput Mater Sci, 1996; 6: 15.
29. Kresse G and Joubert D, From ultrasoft pseudopotentials to the projector augmented-wave method, Phys Rev B, 1999; 59: 1758.
30. Blochl P E, Projector augmented-wave method, Phys Rev B, 1994; 50: 17953.
31. Wood D M and Zunger A, A new method for diagonalising large matrices, J Phys A, 1985; 18: 1343.
32. Johnson D, Modified Broyden's method for accelerating convergence in self-

consistent calculations, Phys Rev B, 1988; 38: 12807.
33. P. Pulay, Convergence acceleration of iterative sequences. the case of scf iteration, Chem Phys Lett.,1980; 73: 393.
34. Perdew J P, Chevary J A, Vosko S H, Jackson K A, Pederson M R, Smgh D J, and Fiolhais C, Atoms, Molecules, Solids, and Surfaces: Applications of the Ge-neralized Gradient Approximation for Exchange and Correlation, Phys Rev B,1992; 46: 6671.
35. Vosko S H, Wilk L and Nusair M, Accurate spin-dependent electron liquid correlation energies for local spin density calculations: a critical analysis, Can J Phys., 1980; 58: 1200.
36. Dudarev S L, Botton G A, Savrasov S Y, Humphreys C J and Sutton A P, Electron-energy-loss spectra and the structural stability of nickel oxide: An lsda+u study Phys Rev B, 1998; 57: 1505.
37. Bengone O, Aouani M, Blochl P and Hugel J, Implementation of the projector augmented-wave LDA+U method: Application to the electronic structure of NiO, Phys Rev B, 2000; 62: 16392.
38. Stephan L, Hannes R and Alex Z, Magnetic interactions of Cr−Cr and Co−Co impurity pairs in ZnO within a band-gap corrected density functional approach, Phys. Rev. B, 2008; 77: 241201.
39. Trimarchi G and Binggeli N, Linear response approach to the calculation of the effective interaction parameters in the LDA+U method, Phys Rev B, 2005; 71: 035101.
40. Monkhorst H J and Pack J D, Special points for Brillouin-zone integrations, Phys Rev 9, 1976; 13: 5188.
41. Jepsen O and Anderson O K, The electronic structure of h.c.p. Ytterbium. Solid State Commun, Solid State Commun., 1971; 9: 1763.
42. Methfessel M and Paxton A T, High-precision sampling for brillouin-zone integration in metals, Phys Rev B, 1989; 40: 3616.
43. Blochl P E, Jepsen O and Andersen O K, Improved tetrahedron method for Brillouin-zone integrations, Phys. Rev. B, 1994; 49: 16223.
44. Ostroukhov A A, Floka V M and Cherepin V T, Surface magnetic moments and electronic structure of Cr(100), Fe(100), and Ni(100) near the Fermi level, Surf. Sci., 1995; 331: 1388.
45. Magaud L, Pasturel A, Mallet P, Pons S and Veuillen J Y, Spin-polarized Shockley state at Ni(111) free surface and at Ni-Cu–based structures on Cu(111) surface, Europhys. Lett., 2004; 67: 90.
46. Frenken J M W, Smeenk R G and Van der Veen J F, Static and dynamic displacements of nickel atoms in clean and oxygen covered Ni(001) surfaces, Surf. Sci., 1983; 135: 147.

How to cite this article: Mohammed YS. Spin polarization of fcc Ni_n (100) and (111) surfaces with GGA and GGA+U. Int J Res Rev. 2015; 2(4):175-182.

****